Determination of Sorption Kinetic Parameters Using the Relaxation-Dependent Solubility Model in the Methanol Vapor—Poly(methyl methacrylate) System

V. Dimos, M. Sanopoulou

Institute of Physical Chemistry, National Center for Scientific Research "Demokritos," GR-15310 Agia Paraskevi, Athens, Greece

Received 7 March 2005; accepted 23 June 2005
DOI 10.1002/app.22817
Published online in Wiley InterScience (www.interscience.wiley.com).

ABSTRACT: The relaxation-dependent solubility model was applied to simulate the experimentally observed sorption kinetic behavior of the PMMA–vapor MeOH system at 25°C, to obtain the main transport parameters. Application of the model in series of successive sorption kinetic runs covering small concentration intervals revealed certain trends in the concentration dependence of the diffusion coefficient of the system, not detectable by a previous simpler analysis of the data. Following excess free volume fill up, relaxation frequencies exhibit a weak exponential dependence on concentration. The functional dependence of the thermodynamic diffusivity on the concentration, deduced from the aforementioned simulation procedure, was tested and found to reproduce reasonably well the series of sorption kinetic runs covering considerably larger concentration intervals. In addition, this analysis indicates a strong dependence of the relaxation mechanism on the concentration interval. © 2006 Wiley Periodicals, Inc. J Appl Polym Sci 100: 2278–2288, 2006

Key words: diffusion; relaxation; swelling; non-Fickian sorption; relaxation dependent solubility model

INTRODUCTION

Determination of the sorption kinetic parameters is of profound importance for the polymer industry. In catalytic polymerization reactions, the polymerization rate will depend on the concentration of the monomers at the catalyst's active sites, thus, solubility and diffusivity of monomers are two of the controlling parameters during a polymerization reaction. Furthermore, design of a great number of polymer products, for instance gas separation membranes, food packaging materials, polymer protective coatings, and bioactive substances controlled release systems, depends on the knowledge of the diffusion coefficient of the corresponding gases and liquids, as a function of their concentration in the polymer phase.

Series of successive sorption kinetic experiments consist of the most common way for the determination of the concentration dependence of the main transport parameters in a glassy polymer-vapor penetrant system, namely the solubility, the diffusion coefficient, and the relaxation frequency. The solubility of the penetrant is easily deduced from the sorbed mass at equilibrium, but the calculation of the remaining kinetic parameters requires a detailed analysis of each experimental kinetic curve, on the basis of theoretical models accounting for the non-Fickian kinetic behavior of these systems. In most of the modeling approaches, non-Fickian kinetics are physically attributed to the coupling of the penetrant diffusion process with the slow viscous relaxation of the swelling polymer and a detailed comparison of theory with results from successive differential sorption experiments has been conducted in several cases. One of the more recent examples in this respect is the work of Durning and coworkers. Thus, in 1990 Mehdizadeh and Durning[1] applied a previously developed model,[2,3] accounting for the time-dependent response of the polymer to diffusion-induced deformation, to predict experimental results of Odani and coworkers for successive differential sorptions of benzene in atactic polystyrene, in the linear limit (i.e., for experiments involving small enough concentration changes to ignore the concentration dependence of the transport properties). The quantitative agreement of the model was reasonable but not perfect. In 1994, Billovits and Durning[4] applied the same model in the case of the poly(styrene)-ethylbenzene system. In the case of two-stage sorption kinetic curves, the initial stage was successfully predicted, while for runs concerning a weight fraction interval exceeding 0.01, the experimental data during the relaxation controlled stage

Correspondence to: V. Dimos (vdim@chem.demokritos.gr).
Contract grant sponsor: Excellence in the Research Institutes Program, GSRT—Greece and EU.

© 2006 Wiley Periodicals, Inc.

approached equilibrium more rapidly than the theoretically predicted ones. The discrepancy was attributed to a weak concentration dependence of the relaxation process during the sorption experiment, not accounted for by the theory. In 1997, Tang et al.[5] reported an efficient numerical solution for the aforesaid linear model.[3] The numerical procedure proved to be accurate and efficient enough for routine analysis of two-stage sorption of the poly(styrene)-ethylbenzene system. In 1997, Huang and Durning[6] compared quantitatively a nonlinear extension of the same model[3] with sorption experiments in the poly(styrene)-ethylbenzene system involving relatively large concentration uptakes, using exponential relationships to capture the strong concentration dependence of the diffusion coefficient and the relaxation times. The theoretical results come in good agreement with the nonlinear behavior experimental data in the liquid state, but the authors concluded that to simultaneously predict the behavior of the system above and below T_g, more accurate representations of the concentration dependence of the transport properties should be used. More recently, Dubreuil et al. have made a detailed analysis of successive differential sorption of toluene in methacrylic copolymers both above and below the glass transition of the mixture,[7,8] based on the model of Long and Richmann.[9] This work focuses on the reliable estimation of the transport parameters of a system, given the various uncertainties of the experimental measurements, using an advanced optimization method.

During a previous experimental work conducted in our laboratory,[10] the kinetic behavior of the methanol–poly(methyl methacrylate) system (MeOH–PMMA) was extensively studied by several series of intervals, as well as integral sorption experiments, at 25°C. A simple kinetic analysis, applicable to sorption experiments covering relatively small concentration intervals (ΔC), was used to deduce constant, polymer fixed diffusivity (D_p) and relaxation frequency (β) values from the corresponding experimental curves. The results indicate that over the concentration (C) range of the series, D_p is a strong (while β a weaker) function of C. In addition, results from a series of experiments covering larger ΔC intervals indicate that β is a strong function of ΔC. In the present study, a more rigorous modeling approach is applied to analyze these data. In particular, the relaxation-dependent solubility (RDS) model developed by Petropoulos[11] is applied to the kinetic runs covering small ΔC intervals, to determine the main transport parameters of the PMMA–MeOH system. Then, the deduced functional dependence of the diffusivity on C is used to test the ability of the model to simulate the kinetic behavior of the system in series of experiments covering larger ΔC intervals, as well as to study the behavior of β with ΔC. Results obtained by the theoretical model are compared with the ones deduced from the simple kinetic analysis mentioned earlier.

THE RELAXATION-DEPENDENT SOLUBILITY MODEL

As already mentioned, non-Fickian sorption kinetics in polymer film–organic vapor systems is usually interpreted in terms of slow viscous relaxation of the swelling polymer, which occurs on time scales comparable with those of the diffusion process. The effect of structural relaxation is mathematically treated by considering the temporal evolution of the polymer swelling as consisting of an "instantaneous" component plus a "delayed" one. Several mathematical models describing the aforementioned evolution exist in the literature.[2,3,6,9,11] In the model proposed by Petropoulos,[11] the diffusion process is formulated in terms of a chemical potential gradient driving force, yielding:

$$\frac{\partial C(x,t)}{\partial t} = \frac{\partial}{\partial x}\left(D_T(C)\ S(a)\ \frac{\partial a}{\partial x}\right) \tag{1}$$

where x represents the distance across a polymer film of thickness $2l$, t is the experimental time, $C(x,t)$ is the local concentration, a is the activity of the penetrant in the membrane, $D_T(C)$ is the thermodynamic diffusion coefficient, and $S(a)$ [$= C/a$] is the solubility coefficient defined as a measure of the sorptive capacity of the polymer at any given stage of the relaxation process. The corresponding boundary conditions for a sorption experiment are as follows:

$$a(x = 0,2l;\ t \geq 0) = a_f \qquad a(0 < x < 2l;\ t = 0) = a_i \tag{2}$$

where a_i and a_f are the initial and final penetrant activity, respectively. The molecular relaxation process is described as follows:

$$\frac{\partial C(x,t)}{\partial t} = \frac{\partial C^q(a)}{\partial a}\frac{\partial a}{\partial t} + \beta(C)\ (C^\infty(a) - C(x,t)) \tag{3}$$

where $\beta(C)$ is the relaxation frequency, as a function of the penetrant concentration, $C^q(a)$ and $C^\infty(a)$ represent the solubility isotherm of the penetrant in the unrelaxed (pseudoequilibrium) and the fully relaxed (equilibrium) polymer, respectively; $C^q(a)$ is defined independently for each sorption experiment over the full range of activity [a_i, a_f], and eq. (3) applies in the range of x. Equation (3) simply states that incremental penetrant uptake (∂C) over a small time interval (∂t) can be analyzed into an "elastic" part, which is associated with a corresponding change in activity ∂a, regarding the unrelaxed polymer matrix; plus a "viscous" part.

The latter corresponds to the amount of penetrant that can be accommodated in the swelling polymer, at constant activity, due to the extra sorptive capacity generated by the relaxation process in time ∂t. Thus, two "sorption equilibrium" isotherms are defined, an instantaneous one [$C^q(a)$], referring to the unrelaxed polymer, in addition to that of the fully relaxed polymer designated by $C^\infty(a)$; the relevant solubility coefficients, for given a, being $S^q = C^q/a$ and $S^\infty = C^\infty/a$. The numerical solution of eqs. (1)–(3), using an explicit finite difference method, is described in detail elsewhere.[11]

Characterization of a sorption kinetic run is achieved by four parameters: the equilibrium sorption isotherm [$C^\infty(a)$], the ratio of the instantaneous to the equilibrium sorptive capacity of the polymer [$\lambda_q = \dfrac{C^q(a_f) - C^\infty(a_i)}{C^\infty(a_f) - C^\infty(a_i)}$], the thermodynamic diffusion coefficient $D_T(C)$, and the relaxation frequency $\beta(C)$.

BRIEF EXPERIMENTAL DATA PRESENTATION

Two membranes of different thicknesses (M51–51 μm and M8–8 μm) were investigated, prepared from solutions of PMMA powder, with an average molecular weight (M_W) of 120,000, supplied by Aldrich (code no. 18,226–5). The membrane preparation procedures and the experimental protocol followed are described elsewhere.[10]

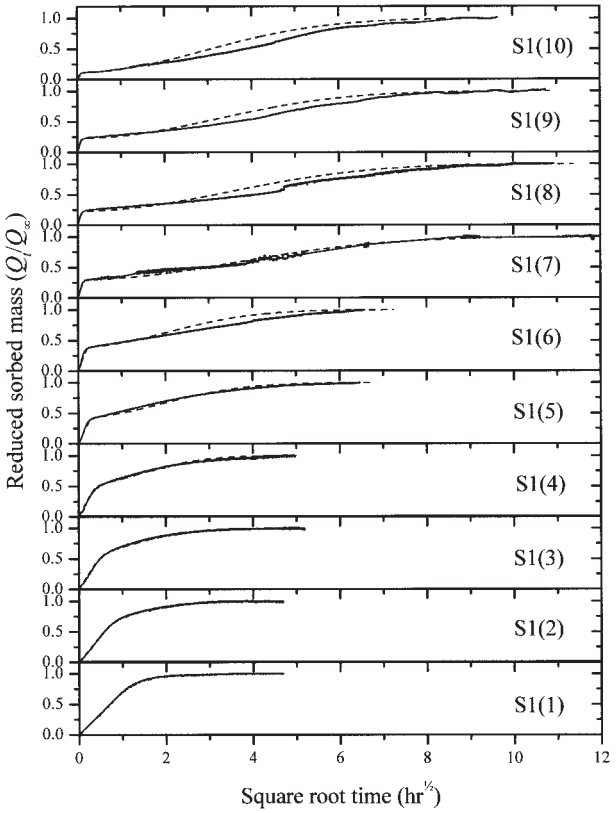

Figure 1 Series S1 of successive absorption runs of MeOH in PMMA film M8 at 25ºC. Continuous lines represent the experimental data,[10] while dashed lines represent the simulation results. $C^\infty(a_f)$ = 0.016 [S1(1)]; 0.027 [S1(2)]; 0.038 [S1(3)]; 0.05 [S1(4)]; 0.062 [S1(5)]; 0.072 [S1(6)]; 0.08 [S1(7)]; 0.095 [S1(8)]; 0.119 [S1(9)]; 0.14 [S1(10)] g/g.

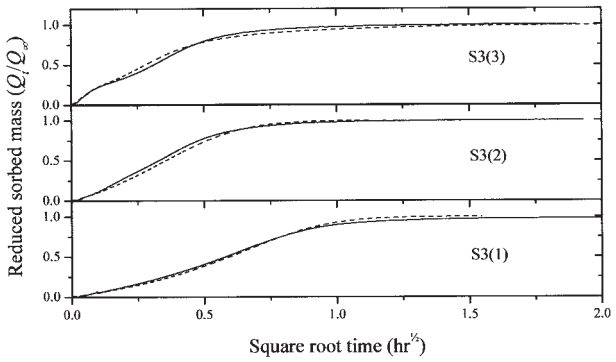

Figure 2 Series S3 of successive absorption runs of MeOH in PMMA film M8 at 25ºC. Continuous lines represent the experimental data,[10] while dashed lines represent the simulation results. $C^\infty(a_f)$ = 0.043 [S3(1)]; 0.085 [S3(2)]; 0.137 [S3(3)]; 0.164 [S3(4)] g/g.

Membrane M8, which was most extensively studied, was initially subjected to series of interval sorption runs. The vapor pressure in all interval series varies in the range of 0–120 Torr, but the size of the pressure interval [corresponding activity interval $\Delta a = a_f - a_i = (p_f - p_i)/p_{sat}$, were p_{sat} is the saturation pressure of MeOH at 25°C] and hence of the concentration interval ($\Delta C = C_f - C_i$) of each run is increased from one series to the next. In the first series (series S1 of Fig. 2 of ref. 10 shown here in Fig. 1) the aforesaid pressure range was covered in 10 successive steps, enabling the study of the system's behavior with increasing C, in experiments covering relatively small ΔC intervals. As shown in the plots of fractional uptake Q_t/Q_∞ *vs.* $t^{1/2}$ (Fig. 1), where Q_t and Q_∞ are the mass uptakes at time t and at the equilibrium, respectively, the kinetic pattern displays a progressive shift from pseudo-Fickian to two stage behavior with increasing C_i. In the following series (e.g., S3 of Fig. 5 of ref. 10 shown here in Fig. 2), the same pressure range was covered in fewer steps (three successive sorption runs for the case of S3), to study the behavior of the system in experiments covering higher ΔC intervals. As the equilibrium sorption data indicated that the sorptive capacity of the film was increased after completion of series S1, attributed to the annealing of the film during S1, a new series (series S5 of Fig. 7 of ref. 10 shown here in Fig. 3) with pressure steps similar to those of S1 was performed, to check the effect of previous sorption history on the study of kinetic behavior. The effect of thickness was also studied in selected interval experiments in the thicker M51 membrane (series S6 in Fig. 3 of ref. 10, shown here in Fig. 4).

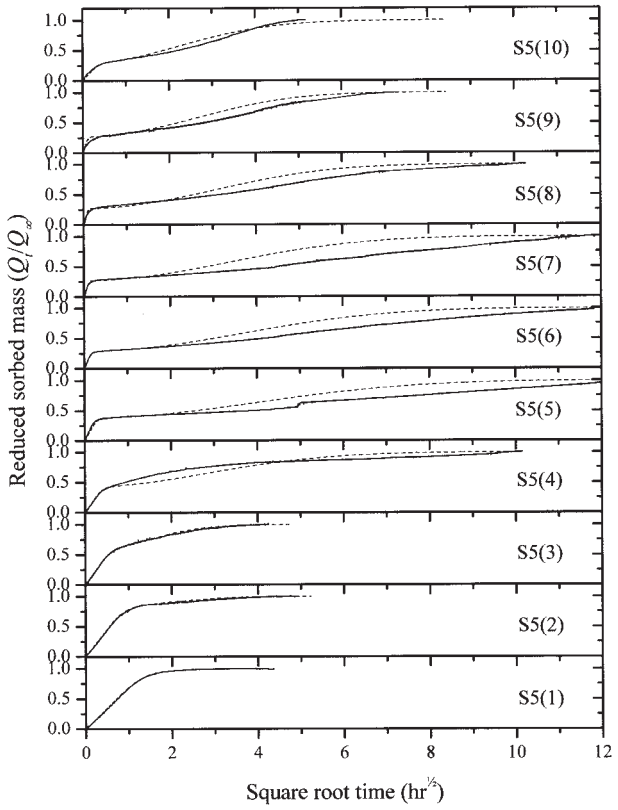

Figure 3 Series S5 of successive absorption runs of MeOH in PMMA film M8 at 25ºC. Continuous lines represent the experimental data,[10] while dashed lines represent the simulation results. $C^\infty(a_f)$ = 0.016 [S5(1)]; 0.026 [S5(2)]; 0.037 [S5(3)]; 0.053 [S5(4)]; 0.069 [S5(5)]; 0.085 [S5(6)]; 0.098 [S5(7)]; 0.120 [S5(8)]; 0.153 [S5(9)]; 0.188 [S5(10)] g/g.

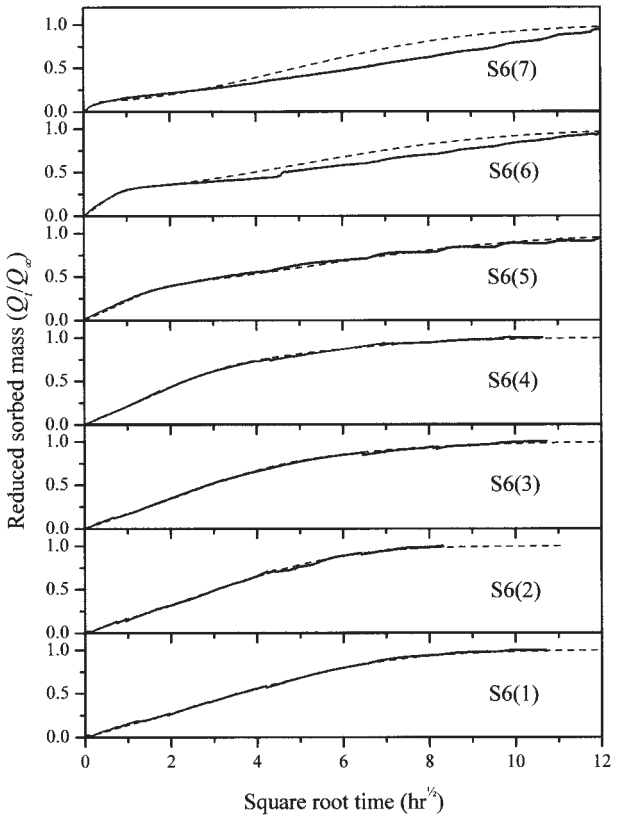

Figure 4 Series S6 of successive absorption runs of MeOH in PMMA film M51 at 25ºC. Continuous lines represent the experimental data,[10] while dashed lines represent the simulation results. $C^\infty(a_f)$ = 0.012 [S6(1)]; 0.021 [S6(2)]; 0.030 [S6(3)]; 0.041 [S6(4)]; 0.059 [S6(5)]; 0.069 [S6(6)]; 0.080 [S6(7)] g/g.

APPLICATION OF THE RDS MODEL TO INTERVAL SERIES OF SORPTION RUNS COVERING SMALL ΔC

Fitting procedure

The model described earlier was first employed to calculate the diffusivity (D_T), the relaxation frequency (β), and the pseudoequilibrium ratio (λ_q) values from the experimental data obtained from series S1, S5, and S6 of interval sorption experiments.[10]

The equilibrium sorption isotherms $C^\infty(a)$ of each series (Fig. 1 of ref. 10, shown here in Fig. 5) were determined experimentally from the equilibrium uptake data Q_∞/M (where M is the weight of the dry polymer membrane). In all cases, $C^\infty(a)$ shows initially a convex upward curvature (associated with absorption in the excess free volume of the glassy polymer matrix), followed by a Flory–Huggins type solution behavior. On the other hand, concerning membrane M8, series S1 displays a different equilibrium sorptive capacity [initial equilibrium sorption isotherm, $C^\infty(a)$, referring to the "as received" polymer] from the one displayed by S3 and S5 (final equilibrium sorption isotherm, $C^\infty(a)$, referring to the annealed polymer), especially in the high activity region. Accordingly, for model calculations each isotherm was approximated by a third order empirical polynomial expression (Ta-

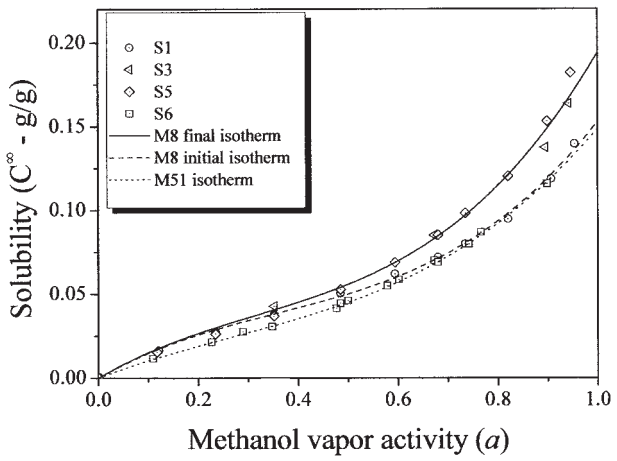

Figure 5 Sorption isotherms of MeOH in PMMA at 25°C. Symbols represent experimental data,[10] and lines represent the polynomial expressions (Table I) used in model simulations.

TABLE I
Sorption Equilibrium Isotherms

	$[C^{\infty} = k_1a^3 + k_2a^2 + k_3a]$[a]
M8 initial (S1)	$0.2483a^3 - 0.2678a^2 + 0.1721a$
M8 final (S5)	$0.2948a^3 - 0.2777a^2 + 0.1768a$
M51 isotherm (S6)	$0.1662a^3 - 0.1325a^2 + 0.1148a$

[a] C^{∞} in g/g.

ble I). This also is the case for the analysis of S6 data. The procedure applied to fit the whole series of kinetic curves is as follows: Diffusivity of MeOH is calculated as a function of concentration, by analyzing iteratively each series of interval sorption runs (S1, S5, and S6). As a first approximation, the constant D_p (polymer fixed diffusion coefficient), β, and λ_q values, previously deduced from each sorption kinetic curve,[10] are used. The method of estimation of these values (described in detail in ref. 10) is best applicable to two-stage curves with well separated first and second stage. In this case, the first stage represents limited sorption according to the instantaneous component of the process and subsequent diffusion in the unrelaxed polymer, up to a pseudoequilibrium concentration value $[C^q(a_f)]$. The second stage represents further sorption up to the equilibrium concentration $[C^{\infty}(a_f)]$, as a result of a pure relaxation process. Accordingly, an estimation of λ_q is obtained from the experimental value of Q_q/Q_{∞}, where Q_q is the amount of penetrant sorbed at the end of the first stage. In ref. 10, a method originally proposed by Park[12] was used to estimate the value of λ_q and a constant value of D_p from the linear part of the reduced sorbed mass plots. As a first approximation, the functional dependence of D_T on C is obtained by fitting these constant D_p vs. C values to an empirical exponential expression with a third-order component. During the determination of the thermodynamic diffusivity curve, the relaxation rate is kept constant and equal to the aforementioned constant value. The whole set of kinetic curves of each series is simulated by the model and a new set of diffusivity values (D_T) is obtained, referred to the initial concentration of each step, so that the theoretical calculated kinetic curves have the same initial slope as the experimental ones. Furthermore, a new λ_q is assumed so that the pseudoequilibrium plateau of both the theoretical and experimental curves coincides. Then, considering only the first step of the interval series and adjusting only the initial slope of the previously calculated diffusivity curve, the value of the thermodynamic diffusion coefficient at zero penetrant concentration (D_0) is iteratively changed and the produced diffusivity function is used to obtain the best fit in the slope of the theoretical and experimental kinetic curves. After D_0 has been deduced, a new diffusivity function is assumed for the whole range of the studied activity, using the obtained D_0 and the previously calculated D_T values for the initial concentration of each step. The whole series of curves is then iteratively simulated, changing the value of the initial diffusivity for the steps that is needed—thus assuming a new diffusivity function—to obtain the best fit in the slope of all the steps simultaneously. Results are displayed in Figure 6.

Following the determination of the thermodynamic diffusivity curve, constant values of β and λ_q are deduced from the experimental data, studying each step independently, by iteratively changing the constant value of β (or λ_q if needed), so that the pseudoequilibrium plateau, the initial slope of the second stage, and the final equilibrium time, are predicted correctly by the theoretically calculated kinetic curves. In the concentration region of two stage curves with well separated first and second stage, the values of constant β deduced from each experiment displayed an exponential dependence on C. Accordingly, in the next simulation procedure, considering the two-stage curves concentration region, a linear function of log β is assumed, and its slope is iteratively changed to obtain the best fit for the initial slope of the second stage and the final equilibrium time, in each step. Results are displayed in Figures 7 and 8. It should be noted that wherever a function of D_T or β is assumed, the quality of the fitting is studied in the whole series of curves simultaneously and not in each one independently.

Quality of sorption kinetic curves fitting

The results of the fitting procedure concerning series S1, S5, and S6 are displayed in comparison with the

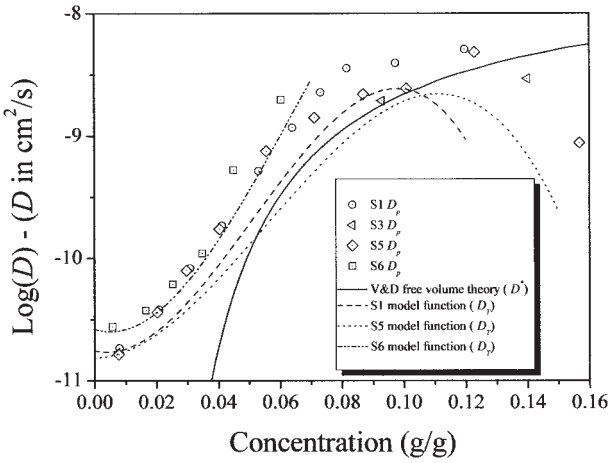

Figure 6 Concentration dependence of the diffusion coefficient of MeOH in PMMA at 25°C. Symbols represent the constant D_p values deduced previously[10] by the method of Park, while dashed lines represent the corresponding exponential functions for D_T (Table III) deduced from model simulation. The D_p values are plotted versus the mean concentration of the first stage.

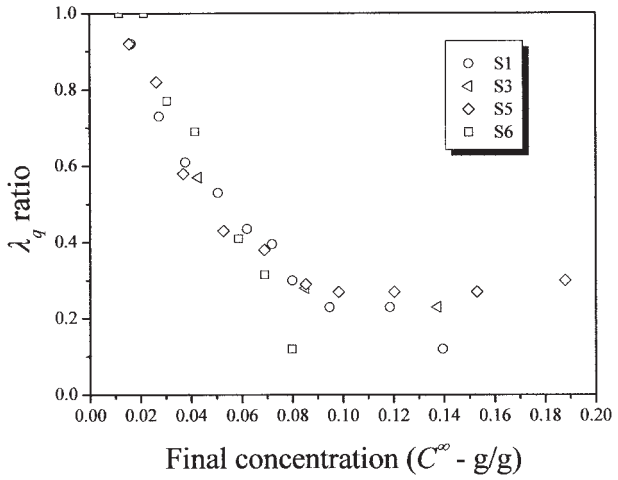

Figure 7 Concentration dependence of λ_q representing the ratio of the instantaneous to the equilibrium sorptive capacity of the polymer, deduced from model simulation of series S1, S3, and S5 in membrane M8 and series S6 in membrane M51.

corresponding experimental sorption kinetic curves (Figs. 1, 3, and 4). In all the three series, the quality of the fitting may be considered very good for the pseudo-Fickian curves (S1R1 to S1R5, S5R1 to S5R3, and S6R1 to S6R5) at the low concentration end, as well as for the first—mainly diffusion controlled—stage of the two-stage curves at the high concentration end. A less satisfactory fitting is observed for the second—mainly relaxation controlled—stage of the two-stage curves. Furthermore, it should be noted that the use of a concentration depended β, as is the case in the results

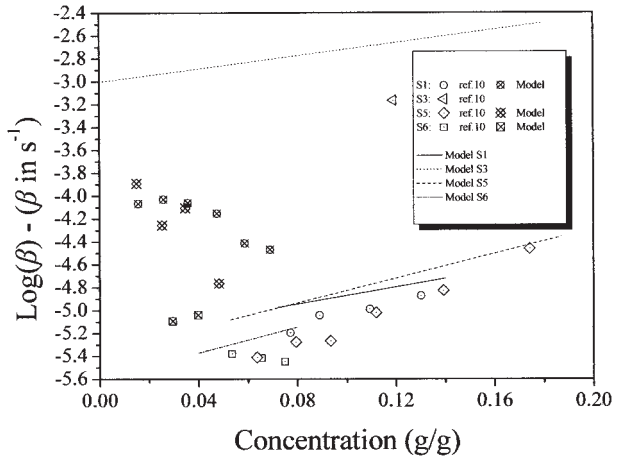

Figure 8 Concentration dependence of the relaxation frequencies of the PMMA–MeOH system at 25°C. Symbols with crosshair represent the constant β deduced from model simulation in the low C end, and lines represent the exponential functions (Table II) deduced by model simulation in the high C end, while dotted symbols represent the constant β values deduced previously.[10]

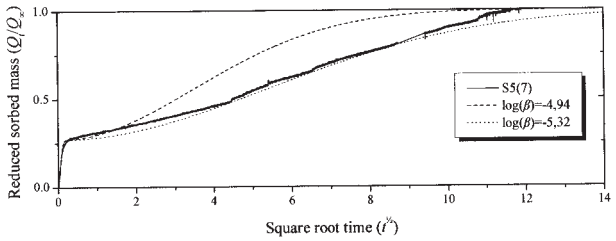

Figure 9 Comparison of model simulation results based on the two different criteria assumed for the 2nd stage fitting of an experimental two-stage curve. Continuous line represents the experimental curve, while dashed and dotted lines represent the final equilibrium time and the whole sorption time scale criteria simulation curves, respectively.

of Figures 1 and 3, did not materially improve the quality of the fitting as compared with the results obtained by the use of a constant β. This is reasonable since the deduced concentration dependence of β is rather weak. As stated earlier, the criterion for a best fit of the second stage was the reproduction of the initial slope of this stage and the correct prediction of the time needed for the equilibrium establishment. This procedure results in most cases in overestimating the mass uptake rate, over extended time periods, of the second stage (runs R8–R10 of series S1 and R5–R10 of series S5). For this reason, a fitting procedure that focuses on the whole sorption time scale of the second stage, while compromising for the final equilibrium time was also employed. Figure 9 represents an example, where the experimental uptake curve of run R7 of series S5 is compared with two theoretical curves representing the best trials to match the second stage, using constant β, on the basis of the two different criteria described earlier. As it can be seen, although a much better representation of the overall second stage rate can be achieved by the second criterion, the model fails to capture the exact curvature of the second stage data, estimating a significant larger time for the equilibrium establishment, indicating that the experimental relaxation process does not strictly follow the kinetic law assumed by eq. (3). Deviations of the second stage relaxation kinetics from eq. (3) have also been observed in other experimental polymer-penetrant systems.[13] Accordingly, it was decided to apply the algorithm in its present form to correctly capture the experimentally observed time of termination of the relaxation process, while compromising for the exact shape of the second stage sorption curve. Surprisingly, deviations of the theoretical from the experimental kinetic curves are more pronounced in the series S5 than those in S1. This leads to the conclusion that the relaxation mechanism of the as received polymer follows a better resemblance to a pseudo first-order kinetic than the annealed polymer.

Estimation of λ_q

The constant λ_q values deduced from each kinetic run of series S1, S5, and S6 are plotted vs. the equilibrium concentration [$C^{\infty}(a_f)$] of each step (Fig. 7). As already discussed, this quantity can be easily identified experimentally only for two-stage curves, with well separated first and second stage. It is quite encouraging that the results of model calculations, from all three series, are practically coincident not only in the concentration region of two-stage curves but also in the low C region that corresponds to pseudo-Fickian curves. The observed trend of λ_q with C^{∞}, depicted in Figure 7, will be analyzed later.

Results on thermodynamic diffusivity isotherm

The diffusivity curves deduced from the model simulations of series S1 and S5, as well as from the S6 one, for the concentration range it applies, display the same trends with rising C (Fig. 6). Thus, an almost linear log D_T vs. C relation is observed in the larger part of the curves. In both cases, the leveling off of the curves in the concentration range 0–0.01 g/g mainly results from the use of nearly constant D_T required for the fitting of the first step, as well as the fact that the initial thermodynamic diffusivity calculated for the second step of each series is almost the same as the one resulted from the corresponding first step (D_0). On the other hand at the high C end, a drop in the diffusivity value is depicted in both S1 and S5 series, mainly produced by the last step of the S1 and the two final runs of the S5 series. The produced maximum in the D_T vs. C curve is more pronounced in the case of series S5, due to the higher concentrations achieved in this series. A possible explanation for this behavior is clustering of methanol molecules at high activities. In general, clustering of penetrant molecules in dense polymeric membranes may result in a decreasing diffusivity with rising concentration, since penetrant clusters are less mobile than monomers, and the phenomenon is not limited to hydrophobic polymer-water systems, in which polymer-penetrant affinity is low. For example evidence of methanol clustering, and concurrent decrease of diffusivity with rising C, has been found in hydrophobic poly(dimethylsiloxane),[14] but also found in a less hydrophobic polyimide polymer.[15] PMMA shows a much higher affinity for methanol compared with PDMS, but similar and even lower as compared with the specific polyimide.[15] This is shown by the estimated sorption capacity of the three polymers for MeOH, in the low activity region (before the onset of clustering), expressed as the ratio $w_{\mathrm{MeOH}}/a_{\mathrm{MeOH}}$, where w_{MeOH} is the weight fraction of the equilibrium sorbed methanol at a_{MeOH}: ~0.007 [Fig. 4 of ref. 14], 0.19 [Fig. 5 of this work], and 0.29 [Table 3 of ref. 15] for the PDMS, PMMA, and the polyimide, respectively.

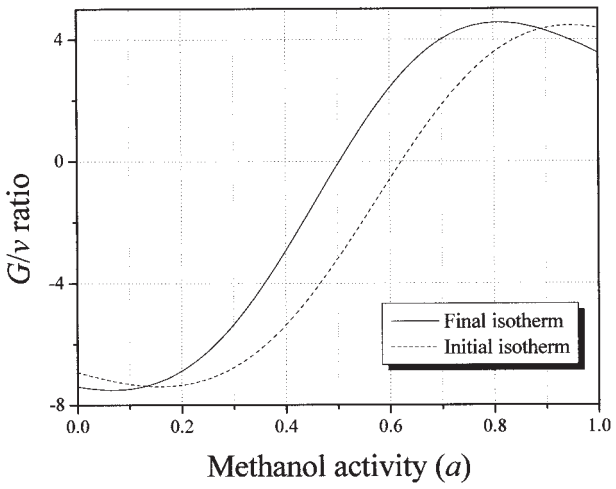

Figure 10 Zimm-Lunberg clustering function for the initial and the final isotherms of the M8 membrane.

The Zimm and Lundberg cluster integral[16,17] provides evidence of MeOH clustering within the polymer matrix. The advantage of this integral is that it can be obtained directly from equilibrium data using the following relation:

$$G/v = -\varphi_p\left[\frac{\partial\left(a_{\mathrm{MeOH}}/\varphi_{\mathrm{MeOH}}\right)}{\partial a_{\mathrm{MeOH}}}\right]_{P,T} - 1 \qquad (4)$$

where G is the cluster integral, v is the methanol partial molar volume, φ_p and φ_{MeOH} are the polymer and MeOH volume fractions, respectively, and a_{MeOH} is the methanol vapor activity. Values of $G/v > 0$ indicate that methanol molecules tend to cluster. Using the solubility isotherms of S1 and S5 series (Table I), one can obtain the quantity G/v as a function of a_{MeOH}. Evidence of methanol clustering is observed for activities higher than 0.6 for S1 and 0.5 for S5 (Fig. 10), but note that these activities refer to approximately the same C (~0.06 g/g).

On a quantitative basis, the S1 and S5 diffusivity curves are practically coincident up to a penetrant concentration of ~0.03 g/g (Fig. 6), which is also the range of coincidence of the corresponding isotherms (Fig. 5). Above this concentration the S5 diffusivity curve shifts to lower values, as compared with the S1 curve, and this discrepancy becomes more pronounced above 0.06 g/g. It is apparent that the sorptive capacity was enhanced after the completion of series S1 (Fig. 5), indicating a more loose structure in the following series (S3 and S5). Accordingly, the lower D_T values obtained by analysis of series S5 kinetic curves may be attributed to an enhanced clustering tendency of methanol molecules.

The diffusivity curve obtained from the thicker M51 membrane is displaced to higher values in comparison

with the S1 and S5 curves. This displacement probably reflects differences in the fine structure of the two films, arising from different preparation conditions,[10] and should be correlated to the sorption isotherm data (Fig. 5). According to the dual mode transport mechanism,[18] the penetrant molecules sorbed in a glassy polymer matrix consist of two distinct populations; one dissolved by a Henry's law mode of dissolution in the dense polymer matrix, and the other adsorbed by a Langmuir mode in the fixed microcavities (constituting the excess free volume of the glassy polymer) dispersed in the said matrix. The Langmuir population is assumed to be totally or partially immobilized and experimental data indicate that the diffusivity of the Langmuir population can be of more than one order of magnitude lower than that of the Henry's law population.[19,20] Since the isotherm data (Fig. 5) indicate that a lower fraction of excess free volume is present in M51 as compared with M8, one may attribute the higher diffusion coefficients observed in the former, to a lower contribution of the Langmuir population to the overall effective diffusion coefficient of the system. In addition, a diffusivity value discrepancy may be partly attributed to the experimental error in the membranes' thickness measurement.

Furthermore, the results of the model application are compared with those previously deduced from the same experimental data[10] by the method of Park,[12] (Fig. 6). As far as series S1 and S5 are concerned, the results from Park's method show the same main trends with C with those of the RDS model: a coincidence of the data of the two series at the low C end and an increasingly higher discrepancy between them at higher C's. Moreover, an indication of a maximum diffusivity at the high C end is discernible, although the later is not well established because of the limited data points available. On the other hand, the diffusion coefficient values from Park's method are systematically higher than those determined by the RDS model. The two sets of results are not strictly comparable, as the constant D_p values deduced by Park's method refer to a polymer-fixed frame of reference in contrast to the RDS results in terms of a thermodynamic diffusivity (D_T). Furthermore, according to eq. (3), the overall uptake rate calculated by the model at each time t during a sorption experiment is based on the increase of $C(x,t)$ due to the diffusion process [first term on the right hand part of eq. (3)] as well as the relaxation process [second term on the right hand part of eq. (3)], the contribution of which is limited, but not negligible, during the first stage. On the other hand, in Park's method, the determination of the diffusion coefficient from the initially linear part of the Q_t/Q_q vs. $t^{1/2}/l$ curve[10] is based on the assumption that this part of the sorption curve is purely diffusion-controlled, and the observed penetrant uptake is exclusively imputed to the diffusion process. As a result, the method tends to overestimate the diffusivity as compared with the corresponding values deduced by the RDS model.

The self diffusion coefficient (D^*) can be calculated according to the free volume theory of Vrentas and Duda[21]:

$$D^* = D_{01} \exp\left(- \frac{\gamma(\omega_1 \hat{V}_1^* + \omega_2 \xi \hat{V}_2^*)}{\hat{V}_f} \right) \tag{5}$$

$$\frac{\hat{V}_F}{\gamma} = \omega_1 \left(\frac{K_{11}}{\gamma}\right)(K_{21} - T_{g1} + T) + \omega_2 \left(\frac{K_{12}}{\gamma}\right)(K_{22} - T_{g2} + T)$$

where D_{01} is an adjustable pre-exponential factor, γ is the free volume overlap factor, ω_1 and ω_2 represent the weight fractions of the penetrant and the polymer, respectively, $\hat{V}_1^*$ and $\hat{V}_2^*$ are the specific critical local free volumes required for a penetrant molecule jump and for a polymer jumping unit displacement, respectively, while $\hat{V}_f$ is the specific average free volume of the mixture, and ξ is the ratio of penetrant to polymer critical molar volumes. T_{g1} and T_{g2} are the glass transition temperatures of the penetrant and polymer, respectively, and k_{11}, k_{12}, k_{21}, and k_{22} are related to the WLF constants of the two components. Theoretical values of D^*, at 25°C, were calculated by application of the eq. (5), with $K_{11}/\gamma = 1.17 \times 10^{-3}$ cm^3/g K, $K_{21} - T_{g1} = -47.9$ K, $\hat{V}_1^* = 0.963$ cm^3/g, $\xi = 0.0675$,[18] $K_{12}/\gamma = 3.05 \times 10^{-4}$ cm^3/g K, $K_{22} = 80$ K, $\hat{V}_2^* = 0.788$ cm^3/g, and $T_{g2} = 388$ K (as an average glass transition temperature calculated for the studied sample).[10] The pre-exponential factor (D_{01}) was found to be 5×10^{-7} cm^2/s. It is apparent that the theoretical values of D^*, which are similar to those of the thermodynamic coefficient calculated by the model application, come in good agreement with the theoretically calculated diffusivity curves, in the concentration region of the two-stage experiments. Significant deviations occur in the region of high concentration range, as the parameters used in the calculation of D^* do not describe the system after the clustering of methanol in the polymer matrix. Furthermore, below the concentration of 0.05 g/g, the concentration dependence of D_T, produced by the model, is less steep than the theoretically predicted one, as expected from the application of free volume theory for the glassy state.[2,10] The lower value of D_{01} assumed in the present study, compared with the similar one referring to the polymer fixed diffusion coefficient presented previously,[10] can be attributed to the differences of the model calculated diffusion coefficient, with the values calculated by the method of Park, as discussed earlier.

Relaxation frequencies

As already mentioned, for each sorption run, constant β values were used as a first approximation during the

TABLE II
Relaxation Frequencies

	Average series ΔC (g/g)	Relaxation frequency $[\log(\beta) = j_1C+j_2]$[a]	$\log(\beta_0)$[a]
S1 series	~0.018	$3.7288C - 5.2438$	−5.2438
S3 series	~0.042	$2.861C - 3.0038$	−3.0038
S5 series	~0.018	$5.402C - 5.3681$	−5.3681
			−5.5953
S6 series	~0.010	$5.6089C - 5.5953$	

[a] β, β_0 in s^{-1}; C in g/g.

fitting procedure of all series. The results from series S1, S5, and S6 indicate a mild dependence of β with C in the two-stage concentration range. Accordingly, an exponential function of β vs. C (Table II, Fig. 8) was assumed in the final fitting attempt, only in this concentration region. The concentration dependence deduced from all the three series is similar. The lower relaxation rates obtained from the thicker membrane experimental data (series S6 in M51) should be attributed to differences in the fine polymer structure of this membrane. The concentration dependencies, deduced by the model application, are also in line with the ones indicated by the constant values (Fig. 6) determined in the previous analysis of the kinetic data.[10] On the other hand, the higher values of the present results reflect the overestimated uptake rates during the larger part of the second stage, as already discussed earlier.

Interestingly, in the low C range, the constant β values deduced from pseudo-Fickian curves are higher than those of the two-stage C region (Fig. 8) and tend to decrease with C. This rather unexpected behavior, which is also quantitatively observed in the corresponding kinetic curves (Figs. 1, 3, and 4), is displayed in the excess free volume filling part of the sorption isotherms and must be related to the complex transport mechanism taking place in this region. Apparently, during the polymer's excess free volume filling, molecular relaxation of the amorphous phase and diffusion in the free volume fixed microcavities cooperate to produce a pseudo-Fickian curve, instead of a two stage one. Molecular relaxation model translates both the aforementioned phenomena to a molecular relaxation mechanism, resulting to higher, than the expected, relaxation rate values, as diffusion in the excess free volume occurs faster than solution due to the relaxation of the polymer matrix. The shift between the coupled diffusion–relaxation mechanisms to a pure molecular relaxation one, can also be observed in the S5R4 curve (Fig. 3), which displays an initial pseudo-Fickian character, but results in a linear sorption rate at later times.

APPLICATION OF THE RDS MODEL IN SERIES OF INTERVAL SORPTION RUNS COVERING LARGE ΔC INTERVALS

To further test the results produced so far by the model, as well as to study the dependence of β on ΔC, the $D_T(C)$ function deduced from series S1 (Fig. 6, Table III), was used as an input, to simulate series S3 on M8 consisting of runs covering ΔC intervals approximately three times larger than those of S1. Series S3 sorption equilibrium data (Fig. 5) indicate that the final sorption equilibrium isotherm should be used, as the polymer film has been annealed during S1. The fitting procedure resulted in similar values of λ_q (Fig. 7), compared with the corresponding ones of series S1, S5, and S6, and a new function of β on C (Fig. 8). The model captures satisfactory both the shape and the rate of the two lower S-shaped curves (Fig. 2), although in the concentration range covered by each of these experiments D_T varies approximately one order of magnitude, as well as those of the third two-stage curve. Apparently, the corresponding β vs. C curve is parallel to those obtained from series with smaller ΔC, but displaced nearly two orders of magnitude on the vertical axis. This displacement reflects the fact that β is a strong function of ΔC, in line with results in other glassy polymer-penetrant systems.[2,13,22] In the present form of the model algorithm [where it is assumed that $\beta = \beta_0 \exp(kC)$, where k is a constant], this dependence is expressed mathematically by the higher value of β_0 determined from series S3 as compared with the β_0 applied in the series of runs covering smaller ΔC intervals (Table III). An alternative representation of the experimental behavior could include a functional dependence of β on both C and ΔC.

TABLE III
Thermodynamic Diffusion Coefficient Isotherms

	Model function $[\log(D_T)=h_1C^3 + h_2C^2 + h_3C + h_4]$[a]	log $[D_T(C = 0)]$
S1 series	$-5198.256C^3 + 793.573C^2 - 6.004C - 10.755$	−10.755
S5 series	$-3087.9C^3 + 512.09C^2 + 0.6414C - 10.815$	−10.815
S6 series	$-4170.9C^3 + 822.02C^2 - 8.0399C - 10.579$	−10.579

[a] D_T in cm^2/s; C in g/g.

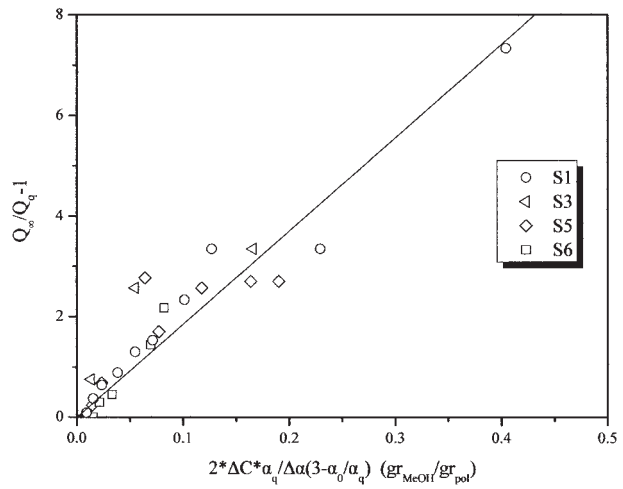

Figure 11 Correlation of the λ_q values deduced from model simulation with activity, according to eq. (6). Linear regression results in a value of 0.7 GPa for the bulk modulus (B).

PSEUDOEQUILIBRIUM RATIO (Λ_Q)

The values of λ_q determined from all four series are practically coincident and drop asymptotically to the value of 0.24, with respect to final concentration (C_f). This behavior is predicted by Newns' approach on the nature of the relaxation process.[23] In his study of two stage sorption of water by cellulose, Newns suggests that the rate of relaxation depends on the magnitude of the osmotic swelling stress induced by the penetrant, the latter being analogous to the amount of penetrant sorbed during the first stage. This treatment predicts that λ_q should decrease with increasing concentration or activity, in keeping with the results obtained by this study (Fig. 7). The relevant equation reads (to a first-order approximation)[23]:

$$Q_\infty/Q_q - 1 = 1/\lambda_q - 1 \approx \frac{2\Delta C\hat{V}_A B a_q}{\Delta a RT\rho_A(3 - a_i/a_q)} \quad (6)$$

where $\hat{V}_A$ is the molar volume of the liquid penetrant (MeOH), B is an elastic bulk modulus, a_q is the activity corresponding to the pseudoequilibrium concentration [$C^q(a_f)$], according to the equilibrium sorption isotherm [$C^\infty(a)$, namely $C^\infty(a_q) = C^q(a_f)$], R is the universal gas constant, T is the experimental temperature, and ρ_A can be approximated by the density of the liquid penetrant (MeOH). Plots of the data deduced from all the series (Fig. 11) reveal a correlation of λ_q and activity in accordance with eq. (6). The slope of the line deduced by a linear regression analysis of the λ_q values of all series, in a plot of $Q_\infty/Q_q - 1$ vs. $\frac{2\Delta C a_q}{\Delta a(3 - a_o/a_q)}$ (Fig. 11), leads to a value of 0.698 GPa for the elastic modulus (B), which is similar to the B value deduced from the same analysis in other glassy polymer-organic vapor systems.[13,22]

SUMMARY AND CONCLUSIONS

The RDS model developed by Petropoulos was applied to simulate the experimentally observed sorption kinetic behavior of the PMMA–vapor MeOH system at 25°C, to obtain the main transport parameters of the system. Third order polynomial empirical equations were used to express the complex, experimentally determined equilibrium sorption isotherm of the system. Application of the model in series of successive sorption kinetic runs covering small ΔC revealed certain trends in the concentration dependence of the main transport parameters of the system, not detectable by a previous simpler analysis of the data. First, to fit the whole series of runs spanning a concentration range of 0–0.8 g/g, exponential empirical functions, with a third order component, were used to represent the peculiarities of the concentration dependence of the diffusion coefficient of the particular system. The said peculiarities mainly consist of a maximum in the D_T vs. C curve, which was attributed to clustering of MeOH at high activities, as also indicated by application of the Zimm and Lumberg clustering function. Differences between the absolute values of diffusivity deduced from the model and from a simpler kinetic analysis were mainly attributed to the simplified assumptions of the latter method, regarding the operation of the relaxation mechanism. Second, the corresponding relaxation frequencies deduced from the fitting procedure, displayed a weak exponential dependence on C at the high C region where two-stage sorption behavior is observed, but were found to decrease with increasing C in the low C region, where pseudo-Fickian behavior prevails. The latter effect probably arises from the complex transport mechanism, operating in the excess free volume filling region of the sorption isotherm. Finally, the quality of the fitting of the second stage of two-stage curves was inferior to that of the corresponding first stage, indicating that the relaxation process does not strictly follow the corresponding first-order kinetic law assumed by the model.

The functional dependence of D_T on C deduced from the aforementioned simulation procedure was tested and found to reproduce reasonably well the series of sorption kinetic runs covering considerably larger concentration intervals. The log β vs. C linear function deduced from this series was approximately parallel to the ones deduced from the series covering smaller ΔC, but displaced to considerably higher β values, reflecting the strong dependence of the relaxation mechanism on the ΔC of the sorption experiment.

A crucial test of the simulation results concerns the quantity λ_q, describing, for each sorption experiment, the ratio of the instantaneous to the equilibrium sorptive capacity of the polymer. The values of λ_q deduced from different series, in two different membranes, were found to be practically the same. Moreover, they were found to decrease with C_f (or the final activity) of the experiment, in a manner predicted by Newns theory on the nature of the relaxation process.

References

1. Mehdizadeh, S.; Durning, C. J. AIChE J 1990, 36, 877.
2. Durning, C. J. J Polym Sci Polym Phys Ed 1985, 23, 1831.
3. Durning, C.J.; Tabor, M. Macromolecules 1986, 19, 2220.
4. Billovits, G. F.; Durning, C. J. Macromolecules 1994, 27, 7630.
5. Tang, P. H.; Durning, C. J.; Guo, C. J; DeKee, D. Polymer 1997, 38, 1845.
6. Huang, S. J.; Durning, C. J. J Polym Sci: Polym Phys Ed 1997, 35, 2103.
7. Dubreuil, A. C.; Doumenc, F.; Guerrier, B.; Allain, C. Macromolecules 2003, 36, 5157.
8. Dubreuil, A. C.; Doumenc, F.; Guerrier, B.; Johannsmann, D.; Allain, C. Polymer 2003, 44, 377.
9. Long, F. A.; Richman, D. J. Am Chem Soc 1960, 82, 513.
10. Dimos, V.; Sanopoulou, M. J Appl Polym Sci 2005, 97, 1184.
11. Petropoulos, J. H. J Polym Sci: Polym Phys Ed 1984, 22, 1885.
12. Park, G. S. Trans Faraday Soc 1961, 57, 2314.
13. Sanopoulou, M.; Roussis, P. P.; Petropoulos, J. H. J Polym Sci Part B: Polym Phys 1995, 33, 993.
14. Favre, E.; Schaetzel, P.; Nguygen, Q. T.; Clement, R.; Neel, J. J Membr Sci 1994, 92, 169.
15. Shi, B.; Feng, C.; Wu, Y. J Membr Sci 2004, 245, 87.
16. Zimm, B. H.; Lundberg, J. L. J Phys Chem 1956, 60, 425.
17. Rodriguez, O.; Fornasiero, F.; Arce, A.; Radke, C. J.; Prausnitz, J. M. Polymer 2003, 44, 6323.
18. Vieth, W. R.; Howell, J. H.; Hsieth, J. H. J Membr Sci 1976, 1, 177.
19. Paul, D. R.; Koros, W. J. J Polym Sci: Polym Phys Ed 1976, 14, 675.
20. Toi, K.; Morel, G.; Paul, D. R. J Appl Polym Sci 1982, 27, 2997.
21. Vrentas, J. S.; Duda, J. L. J Polym Sci: Polym Phys Ed 1977, 15, 417.
22. Sanopoulou, M.; Petropoulos, J. H. Polymer 1997, 38, 5761.
23. Newns, A. C. Trans Faraday Soc 1956, 52, 1533.